Intramolecular Hydrogen-Bonding Interactions in 2-Nitrosophenol and Nitrosonaphthols: Ab Initio, Density Functional, and Nuclear Magnetic Resonance Theoretical Study

Andrew E. Shchavlev*

Division of Applied Informatics, Volga Region Academy of State Service, 23/25 Sobornaya Street, Saratov 410031, Russia

Alexei N. Pankratov

Department of Chemistry, N. G. Chernyshevskii Saratov State University, 83 Astrakhanskaya Street, Saratov 410012, Russia

Venelin Enchev

Institute of Organic Chemistry, Bulgarian Academy of Science, 1113 Sofia, Bulgaria

Received: December 12, 2006; In Final Form: March 2, 2007

Intramolecular hydrogen bonding (IHB) interactions and molecular structures of 2-nitrosophenol, nitrosonaphthols, and their quinone−monooxime tautomers were investigated at ab initio and density functional theory (DFT) levels. The geometry optimization of the structures studied was performed without any geometrical restrictions. Possible conformations with different types of the IHB of the tautomers were considered to understand the nature of the HB among these conformers. The effect of solvent on hydrogen bond energies, conformational equilibria, and tautomerism in aqueous solution were studied. Natural bond orbital analysis was performed to study the IHB in the gaseous phase and in aqueous medium. The NMR ^{1}H, ^{13}C, ^{15}N, and ^{17}O chemical shifts in the gaseous phase and in solution for the studied compounds were calculated using the gauge-including atomic orbitals approach implemented in the Gaussian 03 program package. The optimized geometrical parameters and ^{1}H NMR chemical shifts are in good agreement with previous theoretical and experimental data.

1. Introduction

The importance of intramolecular hydrogen bonds is supported by a wealth of physical and chemical data.[1,2] They contribute in significant ways to the structures, physical properties, and chemical reactivity of the molecules.

The interest to organic nitroso aliphatic and aromatic molecules is provoked by their high toxic properties as well as mutagenic and carcinogenic ones.[3] To understand the influence of nitroso compounds on human organism it is useful to study the nature of their intramolecular hydrogen bonds (IHBs) that play a significant role in various biochemical processes including metabolism. A systematic theoretical study concerning the tautomerism of *o*-nitrosonaphthols has been reported by Krzan et al.[4] The nitroso−oxime tautomeric equilibrium was studied by ab initio molecular orbital (MO) calculations using the Hartree−Fock method. According the authors quinoid form became favored with increasing of ring system size. It has been found for 2-nitrosophenol and 1-nitroso-2-naphthol the nitroso forms to be more stable, but for 9,10-nitrosophenanthrol the oxime form as more stable. The most stable ortho structures possess an intramolecular H bond that appears to be stronger in oxime forms.

The investigations on the molecular structure of 2-nitrosophenol and nitrosonaphthols, and their oxime tautomers by spectroscopic methods[5−7] and ab initio calculations[8−13] indicated considerable intramolecular hydrogen bonding in these molecules. The ab initio calculations performed for 2-nitrosophenol with agreement with the available experimental data confirm the nitroso form as more stable. It was found that the influence of the correlation energy on the relative stabilities is smaller for the rotamers of the nitroso tautomer but substantially for the oxime forms. The structure and conformational equilibrium of the monoximes of 1,2-naphthoquinone have been studied by solid- and liquid-state NMR spectroscopy and nonempirical quantum chemical calculations. The presence of syn and anti oximes of 1,2-naphthoquiinone-2-oxime and two rotameric forms of *syn*-1,2 naphthoquinone-1-oxime in solution is proved by NMR spectroscopy.

The NMR spectroscopy method can be used to characterize the IHB influence in the molecules. The research by quantum chemical calculations and NMR may be applied to explain the structure of such molecules. The solvent effects on different properties including NMR spectra chemical shifts have been taken into consideration. In this connection the solvent effects should be acquired from DFT calculation by the PCM reaction field method.

In connection with the aforementioned, the aim of our explorations is a clarification of the structural properties and IHB nature of 2-nitrosophenol and nitrosonaphthols using modern approaches of quantum chemistry. Correlations between various parameters characterizing the hydrogen bonds are very useful. Particularly useful are the correlations between easily measurable characteristics and those requiring more expensive

* To whom correspondence should be addressed. E-mail: ashch@zmail.ru.

10.1021/jp068540r CCC: $37.00
Published on Web 07/07/2007

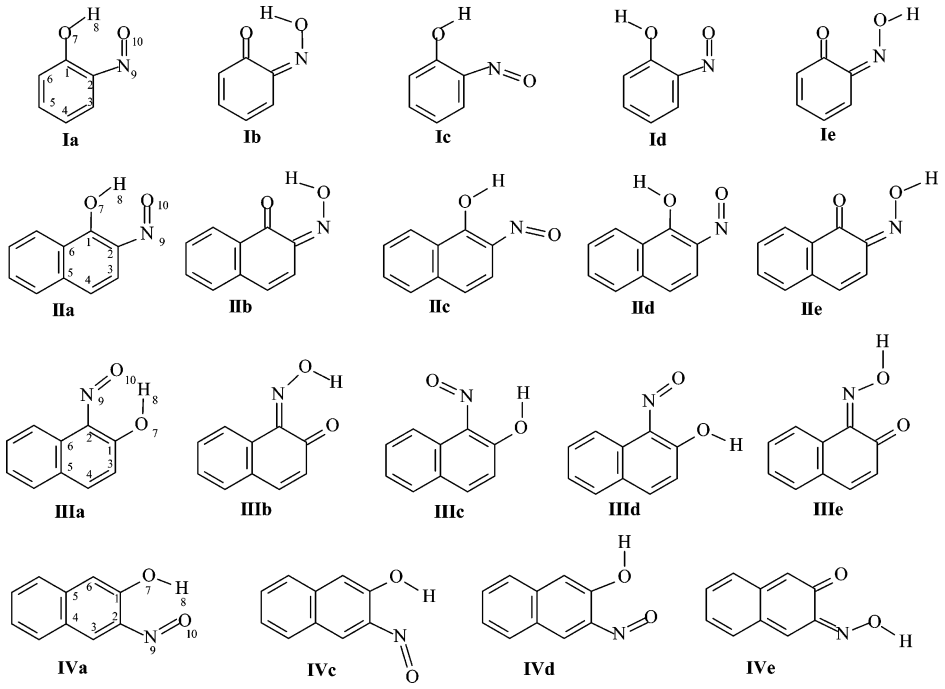

Figure 1. Structure and atom labeling for various forms of 2-nitrosophenol, 2-nitroso-1-naphthol, 1-nitroso-2-naphthol, and 2-nitroso-3-naphthol.

experimental work. In this paper, we theoretically examined the IHB in different positions of nitrosonaphthols molecules and established correlations that allow estimating the strength of IHB.

2. Computational Methods

All calculations of the possible rotamers and tautomers for the 2-nitrosophenol and the nitrosonaphthols in this paper were carried out at ab initio and DFT levels of theory using the Gaussian 98[14] and Gaussian 03[15] packages without any geometrical restrictions. Two different density functionals were used: the hybrid B3LYP functional which combines the three-parameter exchange functional of Becke[16] with the LYP correlation one;[17] the hybrid model called the modified Perdew−Wang one-parameter model for kinetics (MPW1K).[18] The computations were performed using "tight" convergence criteria.[19] The 6-31G(d,p)[20] and 6-311++G(d,p)[21,22] basis set were used. The geometry optimizations were performed at three levels, HF/6-31G(d,p), B3LYP/6-311++G(d,p), and MPW1K/6-311++G(d,p), without geometrical constraints. IHB formation energies have been calculated as the difference between the energy of the compound with *cis*-OH orientation (Figure 1) and that of the *trans*-OH one. No scaling factor for the zero-point energy (ZPE) values has been taken in to account.

The natural bond orbital (NBO) analysis was used to understand the nature of the intramolecular interactions in the studied compounds. NBO analysis has been performed by the NBO 3.1 program.[23] The topological properties of the electron density at the bond critical points (BCPs) have been characterized using the atoms in molecules methodology (AIM)[24] at the B3LYP/6-311++G(d,p) level.

The SCRF method[25] was used to optimize the structures of the nitroso compounds in water solution. In this approach, the solute, treated quantum-chemically, is placed in cavity surrounded by the solvent. The latter is considered as a continuum characterized by such its bulk property as dielectric constant. The standard PCM[26] calculations of the solvation energies with 60 initial tesserae per atomic sphere were performed, and the UAHF[27] model was also applied using the Pauling set of atomic radii.

The ^{1}H, ^{13}C, ^{15}N, and ^{17}O NMR chemical shifts were computed using "gauge-including atomic orbitals" (GIAO) method[28−30] implemented in Gaussian 98/03 programs. The chemical shifts for hydrogen and carbon are the differences of the chemical shielding constants (^{1}H and ^{13}C) of the molecule and the chemical shielding constants of the reference compound tetramethylsilane (TMS, $Si(CH_3)_4$). The differences of the chemical shielding constants of the nitrogen and oxygen atoms in the molecule and the chemical shielding constants of standard compounds (NH_3, H_2O) are predicted chemical shifts for nitrogen (^{15}N) and oxygen (^{17}O). To be comparable, the calculation of the nuclear shielding constants of the reference molecules, TMS, H_2O, NH_3, and the studied molecules were carried out at the same level of theory (B3LYP/6-311++G(d,p)) in the gaseous phase and in solution.

3. Results and Discussion

3.1. Geometry. The geometries of possible conformers for 2-nitrosophenol, **I**, and nitrosonaphthols, **II**, are shown in Figure 1. The selected geometry parameters for all conformers calculated at ab initio and DFT levels of theory are summarized in Table 1. Geometry optimization at RHF ab initio and DFT levels show that all conformers are planar. The deviation of torsional angles for O−H and N−O groups from the plane of benzene and naphthalene rings in the conformers is less than 0.01°. The results thus obtained indicate that all the atoms lie in the plane, which ensures one that the conjugate π-system is extent enough. The O−H bonds are also positioned in the plane that enhances the conjugative effect.

There are no substantial differences of the bond lengths in the aromatic rings of the studied analogues but noticeable differences of O−H and N═O bond length can be seen. The B3LYP/6-311++G(d,p)-calculated $O_{10}-H_8$ bond length in **Ia** is 0.1 Å longer than that in **IIa** and **IIIa**, while the N_9-O_{10} bond length shows the reverse trend. For the tautomers **Ia** and

TABLE 1: Selected Geometrical Parameters for Tautomers and Rotamers of 2-Nitrosophenol (I), 2-Nitroso-1-naphthol (II), 1-Nitroso-2-naphthol (III), and 2-Nitroso-3-Naphthol (IV) Calculated at the B3LYP/6-311++G(d,p) Level in the Gaseous Phase and in Water Solution (in Parentheses) (Distances in Angströms, Angles in Degrees)

compound	C_1-O_7	O_7-H_8	C_2-N_9	N_9-O_{10}	C_1-C_2	H_8-O_{10}	$C_1-O_7-H_8$	$C_2-N_9-O_{10}$	O···O
				2-Nitrosophenol					
Ia	1.333 (1.335)	0.988 (0.988)	1.394 (1.381)	1.240 (1.249)	1.425 (1.429)	1.704 (1.723)	106.7 (107.7)	116.5 (117.1)	2.567 (2.575)
Ib	1.252 (1.257)	1.545 (1.554)	1.320 (1.315)	1.324 (1.334)	1.481 (1.486)	1.017 (1.015)	99.4 (99.9)	117.5 (117.9)	2.487 (2.491)
Ic	1.344 (1.341)	0.973 (0.983)	1.407 1.393)	1.221 (1.232)	1.414 (1.419)		107.6 (117)	117.5 (117.7)	
Id	1.351 (1.341)	0.965 (0.988)	1.433 (1.404)	1.215 (1.230)	1.417 (1.426)		109.3 (110.4)	117.4 (118.6)	2.671 (2.678)
Ie	1.221 (1.233)		1.300 (1.303)	1.361 (1.351)	1.517 (1.511)	0.966 (0.999)		115.7 (116.5)	2.635 (2.653)
				2-Nitroso-1-naphthol					
IIa	1.323 (1.321)	1.002 (1.002)	1.383 (1.369)	1.251 (1.262)	1.416 (1.422)	1.608 (1.620)	105.7 (106.6)	116.8 (117.5)	2.507 (2.512)
IIb	1.245 (1.246)	1.603 (1.606)	1.314 (1.309)	1.335 (1.348)	1.482 (1.489)	1.003 (1.002)	99.7 (100.6)	118.3 (118.6)	2.521 (2.519)
IIc	1.339 (1.331)	0.976 (0.985)	1.398 (1.380)	1.225 (1.239)	1.401 (1.409)		106.9 (111.4)	117.7 (117.7)	
IId	1.345 (1.334)	0.964 (0.980)	1.429 (1.400)	1.216 (1.234)	1.400 (1.414)		110.2 (118.1)	117.8 (119.3)	2.637 (2.629)
IIe	1.217 (1.225)		1.298 (1.300)	1.366 (1.361)	1.514 (1.511)	0.965 (0.989)		115.9 (116.4)	2.621 (2.620)
				1-Nitroso-2-naphthol					
IIIa	1.323 (1.323)	1.003 (1.005)	1.376 (1.361)	1.254 (1.268)	1.419 (1.427)	1.598 (1.594)	105.7 (106.2)	117.2 (117.7)	2.497 (2.493)
IIIb	1.247 (1.252)	1.581 (1.581)	1.309 (1.305)	1.335 (1.347)	1.485 (1.490)	1.006 (1.006)	99.8 (100.5)	118.8 118.9)	2.504 (2.501)
IIIc	1.336 (1.333)	0.979 (0.986)	1.391 (1.374)	1.229 (1.347)	1.413 (1.421)		106.1 (110.3)	120.2 (120.1)	
IIId	1.349 (1.335)	0.965 (0.990)	1.419 (1.389)	1.220 (1.239)	1.403 (1.417)		109.2 (110.6)	117.8 (119.1)	2.609 (2.618)
IIIe	1.219 (1.231)		1.293 (1.295)	1.366 (1.359)	1.518 (1.512)	0.965 (0.988)		116.4 (117.2)	2.595 (2.611)
				2-Nitroso-3-naphthol					
IVa	1.343 (1.348)	0.981 (0.982)	1.400 (1.387)	1.236 (1.245)	1.442 (1.444)	1.751 (1.769)	107.2 (108.1)	116.5 (117.0)	2.602 (2.610)
IVc	1.350 (1.350)	0.972 (0.981)	1.413 (1.398)	1.219 (1.231)	1.431 (1.435)		107.7 (111.4)	117.5 (117.8)	
IVd	1.354 (1.349)	0.965 (0.986)	1.434 (1.408)	1.214 (1.228)	1.436 (1.443)		109.1 (110.1)	117.5 (118.6)	2.627 (2.689)
IVe	1.226 (1.241)		1.305 (1.309)	1.357 (1.343)	1.519 (1.514)	0.966 (0.991)		115.5 (116.4)	2.628 (2.653)

Ib of 2-nitrosophenol in which IHB between OH and NO groups exists the calculated distances are 1.704 Å for $H_8\cdots O_{10}$ in **Ia** and 1.545 Å for $O_7\cdots H_8$ in **Ib**. The calculated O−H···O angles are larger than 120°, and that is favorable for the formation of IHB interaction. The obtained results for the nitrosonaphthols **II-IV** show that the O−H···O distances are remarkably short, between 1.60 and 1.75 Å, and O−H···O angles higher 140°, in agreement with the IHB formation.

The B3LYP/6-311++G(d,p)-computed $O_7\cdots O_{10}$ distance in tautomer **Ia** is 2.567 Å. This value is slightly longer than that in tautomer **Ib**, which is computed to be 2.487 Å, but shorter than the sum of van der Waals radii of oxygen atoms.[31] The contrary trend is observed for tautomers **a** and **b** of the nitrosonaphthols **II** and **III**. The computed $O_7\cdots O_{10}$ distance in conformer **IIa** is 2.507 Å, while in **IIb** this distance increases to 2.521 Å. The same trend is observed in **IIIa** and **IIIb** tautomers. In tautomers **Id**−**IVd** and **Ie**−**IVe** where hydrogen bonding does not exists, the $O_7\cdots O_{10}$ distance is longer in comparison with **Ia**−**IVa** and **Ib**−**IIIb**, species.

The hydrogen bond distance between O···H atoms in **Ia** is computed to be 1.704 Å, which is 0.159 Å longer than that of in **Ib**. Therefore, one may deduce that the predominance of tautomer **Ia** might be caused by the more effective interaction between oxygen and hydrogen atoms through the directional 2p orbital of O_{10} atom even though in **Ia** the O···H distance is somewhat longer than the O···H distance of conformer **Ib**. In the cases of **IIa** and **IIb**, **IIIa** and **IIIb** compounds the differences in O···H distances is about 0.02 Å. The O−H group in **IIa** and **IIIa** is situated 0.02 Å out of the plane of the naphthalene ring while the torsion angle between O−H group and naphthalene ring in **IIb** and **IIIb** becomes near 0°.

In strong hydrogen bonds the distance between the oxygen atoms O···O is 2.40−2.55 Å.[32] According to this criterion, the hydrogen bonds in the compounds studied belong to strong ones.

As can be seen from Table 1 the solvent influences on the geometry of molecules studied. In the aqueous solution, the geometries of **I**−**III** appear to be slightly nonplanar. An elongation by 0.01 Å is observed in the O···O distance going from the gaseous phase to the solution. In aqueous medium the intramolecular hydrogen bond becomes longer by 0.05 Å in **Ia** and by 0.01 Å in **Ib**, and the C_2-N_9 distance becomes shorter by 0.014 Å in **Ia** and by 0.005 Å in **Ib**. There are similar changes for IHB in **IIa**−**IVa** and **IIb** and **IIIb**. For all IHB conformers, the O···H distance is a slightly lengthened in aqueous medium as compared to the gaseous phase. The energy released due to dipole−dipole interaction between polar solvent and solute molecules is sufficient to lose considerable intramolecular forces in solution. Thus the strength of the hydrogen bonding is rather weakened in polar solvent (section 3.2).

3.2. Relative Stability of Rotamers and Tautomers of 2-Nitrosophenol and Nitrosonaphthols. IHB Energy. The values of the calculated total and relative energies at the ab initio and DFT levels for several possible conformers of 2-nitrosophenol and *o*-nitrosonaphthols are summarized in Table 2. The ab initio and DFT calculation results are not much different from each other. For 2-nitrosophenol, the species **Ia** is more stable than the others. In general, all the calculations show that the relative stability of these five forms is in order **Ia** > **Ic** > **Ib** > **Id** > **Ie** in the gaseous phase. Especially, the electron correlation effect at the DFT levels makes the energy difference between conformers **Ia** and **Ic** sensitively increased as compared with ab initio MP4//MP2 level. As can be seen from Table 2, the **Ic** molecule is more stable in comparison with **Ib**. One can be inferred that the rotation of N═O bond is thermodynamically and kinetically favorable[10,11] as compared with proton transfer **Ia** → **Ib**. The stability of **Ic** may be attributed to the Coulombic interaction between positively charged nitrogen atom and negative charged oxygen (section 1.3). The relative stability order is: **Ia** > **Ic** > **Id** > **Ib** > **Ie** (Table 2). The comparing of the results for the gaseous phase and aqueous solution, testify that the O−H bond rotation in aqueous medium is a thermodynamically preferable than hydrogen proton transfer from **Ia** to **Ib**. The contribution of the above-mentioned Coulombic interaction between nitrogen and oxygen atoms to **Ic** stability is much increased taking into account solvent polarization effect in solution (section 1.3).

The relative stability order of the possible 2-nitroso-1-naphthol and 1-nitroso-2-naphthol forms is different from those of 2-nitrosophenol. For 2-nitroso-1-naphthol the order is **IIb** > **IIa** > **IIc** > **IIe** > **IId** and **IIb** > **IIe** > **IIa** > **IIc** > **IId** in the

TABLE 2: Relative Energies (kcal/mol) for the Tautomers and Rotamers of 2-Nitrosophenol (I), 1-Nitroso-2-naphthol (II), 2-Nitroso-1-naphthol (III), and 2-Nitroso-3-Naphthol (IV) in the Gaseous Phase and in Aqueous Solution (Values in Italics) Including ZPE Correction at Different Levels of Theory

computational level	Ia	Ib	Ic	Id	Ie
HF/6-31G(d,p)	0.00	6.13	0.71	8.13	11.62
MP4/6-31G(d)//HF/6-31G(d,p)	0.00	3.06	1.22	8.68	9.24
MPW1K/6-311++G(d,p)	0.00	5.04	2.02	10.24	14.28
B3LYP/6-311++G(d,p)	0.00	3.35	2.80	11.01	12.41
	0.00	*2.92*	*0.62*	*2.79*	*4.60*
	IIa	IIb	IIc	IId	IIe
HF/6-31G(d,p)	3.23	0.00	3.36	15.08	4.76
MP4/6-31G(d)//HF/6-31G(d,p)	4.91	0.00	5.89	16.87	5.34
MPW1K/6-311++G(d,p)	1.79	0.00	3.94	15.70	7.21
B3LYP/6-311++G(d,p)	2.22	0.00	4.50	16.91	7.11
	2.59	*0.00*	*2.85*	*10.18*	*1.09*
	IIIa	IIIb	IIIc	IIId	IIIe
HF/6-31G(d,p)	2.58	0.00	4.83	12.67	5.39
MP4/6-31G(d)//HF/6-31G(d,p)	4.17	0.00	6.87	14.86	5.88
MPW1K/6-311++G(d,p)	1.21	0.00	3.30	14.10	7.66
B3LYP/6-311++G(d,p)	1.54	0.00	4.88	15.41	8.30
	1.95	*0.00*	*3.79*	*7.33*	*1.85*
	IVa	**IVb**	**IVc**	**IVd**	**IVe**
HF/6-31G(d,p)	0.00	15.98	1.12	6.89	22.82
MP4/6-31G(d)//HF/6-31G(d,p)	0.00	11.28	1.35	7.42	18.72
MPW1K/6-311++G(d,p)	0.00		2.79	9.64	18.93
B3LYP/6-311++G(d,p)	0.00		2.80	10.03	20.38
	0.00		*1.56*	*2.63*	*12.24*

gaseous phase and in aqueous solution, respectively. The similar result was obtained for 1-nitroso-2-naphthols. The **IIe** conformer is more stable in energy than **IIb** in aqueous polar solution. This result may be attributed to that the process of the O−H bond rotation **IIb** ⇄ **IIe** and **IIIb** ⇄ **IIIe** is more thermodynamically favorable than hydrogen proton transfer **IIb** → **IIa** and **IIIb** → **IIIa**. On the other hand, the energy difference between conformers **IIa** and **IIc** is computed to be 0.3 kcal/mol and that one between conformers **IIIa** and **IIIc** is calculated to be 1.8 kcal/ mol.

The comparison of the energy differences between conformers of 2-nitroso-3-naphthol shows that the oxime structure **IVb** of 2-nitroso-3-naphthol does not exist, in the calculation process proton moved to O_7 atom. The relative stability of these four conformers follows the order: **IVa** > **IVc** > **IVd** > **IVe**. The order and magnitude of relative energies is similar to the energy differences between **Ia**, **Ic**, **Id**, and **Ie** of 2-nitrosophenol calculated at DFT levels.

The energy of hydrogen bond was estimated by the comparison of the energies of the conformer with hydrogen bond and the rotamer, in which the hydroxy group is turned at 180° to the C−O bond, which should prevent the hydrogen bonding. The computed differences in energy between the "open" and "closed" forms for different structures **I**−**IV** are presented in Table 3.

It is obvious that hydrogen bond energy formation for nitroso tautomeric forms is a larger than for oxime ones. The hydrogen bond energy is reduced with increase of the solvent polarity. For example, the energy of hydrogen bonding in water is decreased by about 60% with respect to the gaseous phase. It is a result of a strong augmentation of the attractive electrostatic terms and solvent polarization which diminish the energy gap between the "closed" and "open" conformers with the consequent weakening of the hydrogen bond energy.[33]

3.3. Electron NPA Charge Distribution and Dipole Moments. To investigate the nature of IHBs in studied target molecules more rigorously, we have performed natural population analysis[34] for 2-nitrosophenol and nitrosonaphthols at B3LYP/6-311++G(d,p) level. Total atomic charges for the possible conformers and tautomers for 2-nitrosophenol, as well as nitrosonaphthols, are summarized in Table 4.

As can be seen, the charge of the hydrogen atom H_8 in the hydroxy group in **I**−**IVa** and **Ib**−**IIIb** has a positive increase at the IHB forms. Also, it may be testified that the charges on oxygen atoms O_7 and O_{10} (**Ia**, **IIa**, **IIIa**, **IVa**) gain additional negative charge as the IHB (O−H···O) forms. One can see a shift of electron density from aromatic system to O_7 with simultaneous shift of electron density to O_{10} through O−H···O bridge. In the case of **Ib**−**IIIb**, the charge on O_7 is negatively increased and the one on O_{10} is a little decreased upon hydrogen bonding. The charge on N_9 is positively decreased going from **Id** to **Ia** and positively increased going from **Ie** to **Ib**. From the data obtained, one can see that IHB makes the hydroxy groups of conformers with IHB more polar than those of conformers where hydrogen bond is absent.

According to the gas-phase computations, during the proton transfer (**Xa** → **Xb**; X = **I**−**III**), the positive charge on the hydrogen atom H_8 of O−H group decreases while its adjacent oxygen O_7 loses some negative charge and O_{10} gains one. As for the nitrogen atom, it gets additional negative charge during the proton transfer. In this way, the interaction of charges on labile hydrogen and oxygen atoms enhances in the course of the reaction thus favored. The charge distributions of exploring structures are altered in the presence of a solvent reaction field.

By use of the PCM model, the charge distributions in the studied structures are found to be influenced by dielectric medium. It is interesting to note that the electron distributions on the O_{10} and N_9 atoms within the PCM are perturbed by the reaction field. Hence, as can be referred above, the interatomic distances would be effected by solvent. To check the relation of interatomic distances from charge electron distributions in different environment, we have built the linearity analysis for **Ia**−**IVa** compounds. Linearity analysis shows that the differences between charges on labile hydrogen H_8 and acceptor oxygen ($Q_H - Q_O$) are linear with geometry parameters (O···H) in the gaseous state and in solution. The correlation coefficients are 0.9981 (gaseous phase) and 0.9996 (aqueous solution), respectively, shown in Figure 2.

The comparison of the data from Table 5 shows that the dipole moments are less sensitive to the calculation level. The calculated dipole moments for the **Ib**−**IIIb** tautomers are higher than for **Ia**−**IIIa**. The differences of dipole moments between all the species in solution are more pronounced than those in the gaseous phase. The relatively higher dipole moments of **Ib**−**IIIb** represent a premise for the latter's predominant stabilization in water solution in comparison to **Ia**−**IIIb**.

3.4. MOs. The MOs were obtained at B3LYP/6-311++G(d,p) level of theory. The lowest-unoccupied MOs (LUMO) and the highest-occupied MOs (HOMO) for **Ia**−**Ic** are shown in Figure 3, and these for structures **a**−**c** of compounds **II** and **III** are shown in Figure 4. In general, both HOMO and LUMO orbitals are of π type; however, their phases are not equal for the molecules **Ia**, **Ib**, and **Ic**. Indeed, the contour in Figure 3 shows the maximum of electron density on aromatic ring in **Ib**. In the case of **Ia** and **Ic**, all electron density is disposed in the region of the O···H···O interaction. In **Ia** (HOMO) it can see the noticeable σ-antibonding interaction and π-antibonding interaction (LUMO) between the nitrogen and oxygen atoms.

TABLE 3: IHB Energy Formation (kcal/mol) for Different Structures of 2-Nitrosophenol and Nitrosonaphthol in the Gaseous Phase and Aqueous Solution Including ZPE Correction at Different Levels of Theory

compound	HF/6-31G(d,p)	MPW1K/6-311++G(d,p)	B3LYP/6-311++G(d,p)	B3LYP/6-311++G(d,p) (in water)
Ia	8.13	10.24	11.01	2.79
Ib	5.48	9.24	9.06	1.67
IIa	11.84	13.91	14.68	7.59
IIb	4.76	7.21	7.11	1.09
IIIa	10.09	12.89	13.88	5.38
IIIb	5.39	7.66	8.30	1.85
IVa	6.89	9.64	10.03	2.63
IVb	6.84			

TABLE 4: Total Atomic Charges (NPA) for the Possible Forms of 2-Nitrosophenol and Nitrosonaphthols in the Gaseous Phase and in Aqueous Solution (in Brackets) Calculated at the B3LYP/6-311++G(d,p) Level

	2-nitrosophenol									
atom	**Ia**		**Ib**		**Ic**		**Id**		**Ie**	
C_1	0.375	(0.382)	0.445	(0.459)	0.376	(0.388)	0.350	(0.369)	0.448	(0.460)
O_7	−0.644	(−0.659)	−0.613	(−0.652)	−0.652	(−0.673)	−0.624	(−0.650)	−0.512	(−0.604)
H_8	0.497	(0.508)	0.481	(0.488)	0.498	(0.527)	0.465	(0.528)	0.472	(0.531)
C_2	−0.030	(−0.022)	0.022	(0.048)	−0.029	(−0.029)	−0.011	(−0.018)	0.070	(0.066)
N_9	0.078	(0.050)	−0.014	(−0.023)	0.027	(0.030)	0.066	(0.037)	−0.069	(−0.062)
O_{10}	−0.389	(−0.437)	−0.448	(−0.486)	−0.318	(−0.395)	−0.294	(−0.384)	−0.469	(−0.501)
	2-nitroso-1-naphthol									
	Iia		**IIb**		**IIc**		**IId**		**IIe**	
C_1	0.433	(0.451)	0.497	(0.514)	0.446	(0.469)	0.413	(0.445)	0.495	(0.511)
O_7	−0.639	(−0.641)	−0.609	(−0.633)	−0.652	(−0.661)	−0.617	(−0.541)	−0.517	(−0.587)
H_8	0.496	(0.505)	0.481	(0.489)	0.497	(0.531)	0.470	(0.528)	0.470	(0.527)
C_2	−0.034	(−0.021)	0.029	(0.060)	−0.038	(−0.036)	−0.028	(−0.032)	0.074	(0.073)
N_9	0.066	(0.028)	−0.009	(−0.058)	0.011	(0.007)	0.060	(0.025)	−0.083	(−0.089)
O_{10}	−0.411	(−0.470)	−0.467	(−0.509)	−0.333	(−0.424)	−0.301	(−0.398)	−0.480	(−0.518)
	1-nitroso-2-naphthol									
	IIIa		**IIIb**		**IIIc**		**IIId**		**IIIe**	
C_1	0.404	(0.420)	0.461	(0.475)	0.408	(0.427)	0.366	(0.396)	0.453	(0.467)
O_7	−0.633	(−0.643)	−0.605	(−0.645)	−0.646	(−0.659)	−0.615	(−0.644)	−0.510	(−0.599)
H_8	0.494	(0.502)	0.480	(0.487)	0.496	(0.526)	0.465	(0.530)	0.469	(0.526)
C_2	−0.009	(0.005)	0.056	(0.086)	−0.004	(0.000)	0.004	(−0.002)	0.080	(0.076)
N_9	0.054	(0.022)	−0.018	(−0.054)	−0.004	(−0.013)	0.049	(0.020)	−0.096	(−0.090)
O_{10}	−0.414	(−0.479)	−0.466	(−0.507)	−0.349	(−0.436)	−0.305	(−0.411)	−0.476	(−0.513)
	2-nitroso-3-naphthol									
	IVa		**IVb**		**IVc**		**IVd**		**IVe**	
C_1	0.347	(0.343)		0.355	(0.358)	0.339	(0.341)	0.435	(0.436)	
O_7	−0.659	(−0.682)		−0.660	(−0.688)	−0.632	(−0.675)	−0.526	(−0.537)	
H_8	0.495	(0.506)		0.490	(0.521)	0.466	(0.524)	0.472	(0.534)	
C_2	−0.012	(−0.007)		−0.015	(−0.016)	0.004	(−0.001)	0.075	(0.071)	
N_9	0.077	(0.052)		0.032	(0.034)	0.064	(0.039)	−0.061	(−0.044)	
O_{10}	−0.379	(−0.427)		−0.314	(−0.384)	−0.291	(−0.377)	−0.459	(−0.484)	

The contour also shows the weak σ-antibonding interaction (HOMO) and π-antibonding interaction (LUMO) between the O···O orbitals. For **Ib**, the contour shows the σ-bonding interaction (HOMO) and π-antibonding interaction (LUMO) between the O···O orbitals. As to **IIIa**−**IIIc** systems, then their MO (HOMO−LUMO) shapes in many respects are analogous to **Ia**−**Ic** systems. The HOMO orbital of **IIa** system is primarily of $C_1-C_2-N_9$ and C_3-C_4 π-bonding character, in addition to the C_1-O_7 and N_9-O_{10} π-antibonding contribution. The interaction between O_7 and O_{10} oxygen atoms has a π-bonding character. For **IIb** structure, the electronic rearrangements induced by ground state proton transfer lead to shift of electron distribution from C_1 to N_9-O_{10} bond, and the $O_7\cdots O_{10}$ interaction has also π-bonding character. On the other hand, the LUMO orbitals for **IIb** compound also present C_1-O_7 and N_9-O_{10} π-antibonding character like the HOMO orbital but with some $C_6-C_1-C_2$ bonding character and the obvious $O_7\cdots O_{10}$ π-antibonding contribution on the IHB system. The LUMO orbitals of **Ia** and **IIa** (Figure 5) possess a high projection on the O_{10} atom and a null projection on the O_7 atom (in the same way to the HOMO), whereas for **IIIa** (Figure 5), the LUMO orbital presents slightly higher projection on the O_{10} atom and lower projection on O_7 than that for the respective oxygen atoms of the HOMO orbitals. After tautomerization, the LUMO orbital of the **IIb** and **IIIb** still exhibits a large electron density projection on the O_{10} atom, and almost null projection on the O_7 atom, thereby favoring the proton-transfer process. In contrast, for **Ib** the LUMO orbital shows a substantial electron density projection on the O_7 atom, and thus the **Ia** → **Ib** proton transfer is hindered. Thus, we may explain why **Ia**, **IIb**, and **IIIb** are enthalpically preferred in studied series of our compounds.

We have also examined how the relative energies of the orbitals (HOMO−LUMO gap) in each molecule respond to changes in their ground states. For example, the energy differences HOMO−LUMO is 0.119 a.u. in **IIIa**. This is a

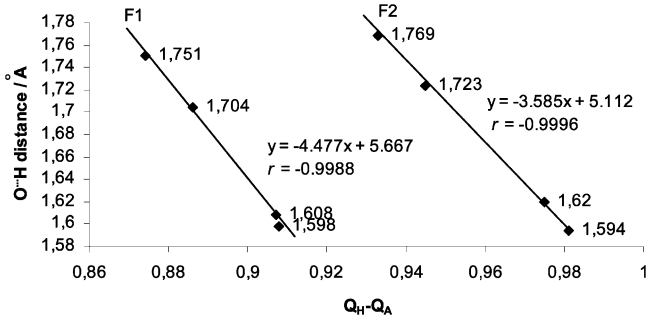

Figure 2. Correlation of O···H distances in **Ia**−**IVa** with Q_H-Q_A; F1 (gaseous phase) and F2 (aqueous solution). The calculations are carried out at B3LYP/6-311++G(d,p) level.

TABLE 5: Dipole Moments (*D*) for Different Structures of 2-Nitrosophenol and Nitrosonaphthols in the Gaseous Phase and in Solution (in Italics)

method	Ia	Ib	Ic	Id	Ie
MPW1K/6-311++G(d,p)	3.42	4.13	2.95	5.11	3.12
B3LYP/6-311++G(d,p)	3.75	4.16	3.27	5.33	3.13
B3LYP/6-311++G(d,p)	*5.56*	*6.16*	*4.827*	*8.27*	*4.69*
	IIa	**IIb**	**IIc**	**IId**	**IIe**
MPW1K/6-311++G(d,p)	4.18	4.79	3.84	5.87	2.51
B3LYP/6-311++G(d,p)	4.64	4.90	4.34	6.14	2.67
B3LYP/6-311++G(d,p)	*7.19*	*7.43*	*6.77*	*9.67*	*4.11*
experiment[45]	4.21				
	IIIa	**IIIb**	**IIIc**	**IIId**	**IIIe**
MPW1K/6-311++G(d,p)	4.05	4.78	3.87	5.23	3.71
B3LYP/6-311++G(d,p)	4.41	4.79	4.06	5.46	3.75
B3LYP/6-311++G(d,p)	*6.99*	*7.32*	*6.36*	*9.02*	*5.69*
experiment[45]	4.19				
	IVa	**IVb**	**IVc**	**IVd**	**IVe**
MPW1K/6-311++G(d,p)	4.11		3.27	5.34	3.80
B3LYP/6-311++G(d,p)	4.44		3.75	5.53	3.81
B3LYP/6-311++G(d,p)	*6.79*		*5.46*	*8.66*	*6.15*

smaller than the 0.13 a.u. HOMO−LUMO gap in **IIIb**. The situation for other compounds is quite similar. The HOMO−LUMO gap for oxime compounds is a few larger than for their nitroso species.

In general, from all our consideration we may suggest that the hydroxy group−nitroso group interaction shifts the electron density from hydroxy group toward the nitroso group, and this shift leads to greater electron redistribution and, consequently, stronger hydrogen bonding.

3.5. NBO and AIM Electron Density Analysis at BCP. The NBO analysis of the IHB for our structures was carried out in the gaseous phase and in aqueous solution. The results are presented in Table 6. The stabilization energies were estimated by analyzing the interactions between the "filled" Lewis-type NBOs and the "empty" non-Lewis NBOs. Our findings are indicative of the occurrence of interactions resulting in a small electron density transfer from the localized NBOs of the idealized Lewis structure into the empty non-Lewis orbitals.

Inspection of Table 6 shows that there is a strong hydrogen bonding interaction in **IIIa**, and its second-order interaction energy is 49.19 kcal/mol ($n_O(\pi) \rightarrow \sigma^*_{O-H}$). Obviously, the hydrogen bond in **IIIa** is stronger than that in others. The charge transfer interaction in the backward direction is the smallest. That is to say, the recombination activities of **IIIa** can be performed effectively and lead to strong interaction, namely, the cooperative effect. Moreover, the charge transfer from π orbital to the antibonding σ^*_{O-H} orbital occurs for **Ia**, **Ib**, **IIa**, **IIb**, **IIIa**, **IIIb**, and **IVa**. Also, the $n_O(\pi) \rightarrow \sigma a$ interaction is much larger than the $n(\sigma) \rightarrow \sigma^*$ one. Such results allow saying taking place in O···H−O. In the case of N···H−O interactions, the σ-type one does exist.

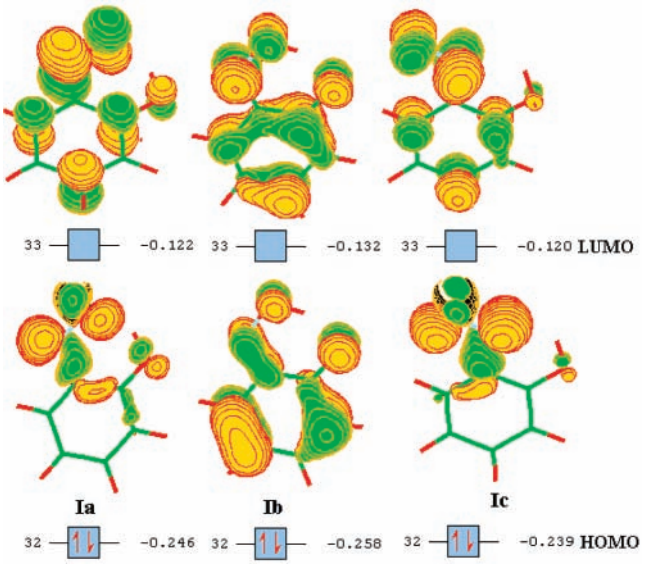

Figure 3. Schematic diagram of molecular orbitals with absolute orbital energies (a.u.) within B3LYP/6-311++G(d,p) computations for different forms of 2-nitrosophenol.

The NBO analysis in solution shows the decreasing of second-order interaction energy $\Delta E_{ij}^{(2)}$ to about 1.5 kcal/mol as compared with the gaseous phase. The exclusion may be fulfilled for **IIIa** and **Ic**, **IIc**, **IIIc** (perceptible changes of second-order interaction energy). The second-order interaction energy comparison between nitroso and oxime forms of 2-nitrosophenol and nitrosonaphthols reveal that nitroso one in a favor.

We have further proceeded with the NBO energetic deletion analysis.[23] Standard NBO energetic deletion analysis is performed by deleting specified elements from the NBO Fock matrix, diagonalizing this new Fock matrix to obtain new density matrix, and passing this density matrix to the SCF routines for a single pass through the SCF energy evaluator. The difference between the energy obtained by such "deletion" procedure and the energy obtained from starting density matrix is a good estimation of the total energy contribution of the deleted terms. By use of this approach, we have removed all Fock matrix elements between high occupancy NBOs of the donor unit to the low occupancy NBOs of the acceptor unit, which corresponds to removing the effects of inter-fragment delocalizations between O···H−O in studied compounds. The results are summarized in Table 6. The strongest effect of the above delocalizations is observed for monooxime structures. Of course, the last conclusion about the degree of effects of all intermolecular delocalizations is not to be taken in an absolute quantitative sense. They are valuable only in the course of estimating the relative contributions to the total energy of interfragment delocalizations and not of the overall contribution to the total interaction energy. This is so since, first of all, a single SCF step through which the new density matrix is passed does not lead to a full SCF convergence. The symbate behavior of the energy change ΔE_{DEL} from the NBO energetic deletion analysis and the second-order perturbation energy $\Delta E_{ij}^{(2)}$ allows the linear relation between them to be assumed. Thus, a good correlation ratio has been received between the ΔE_{DEL} and $\Delta E_{ij}^{(2)}$. The result is shown in Figure 7. The regression analysis

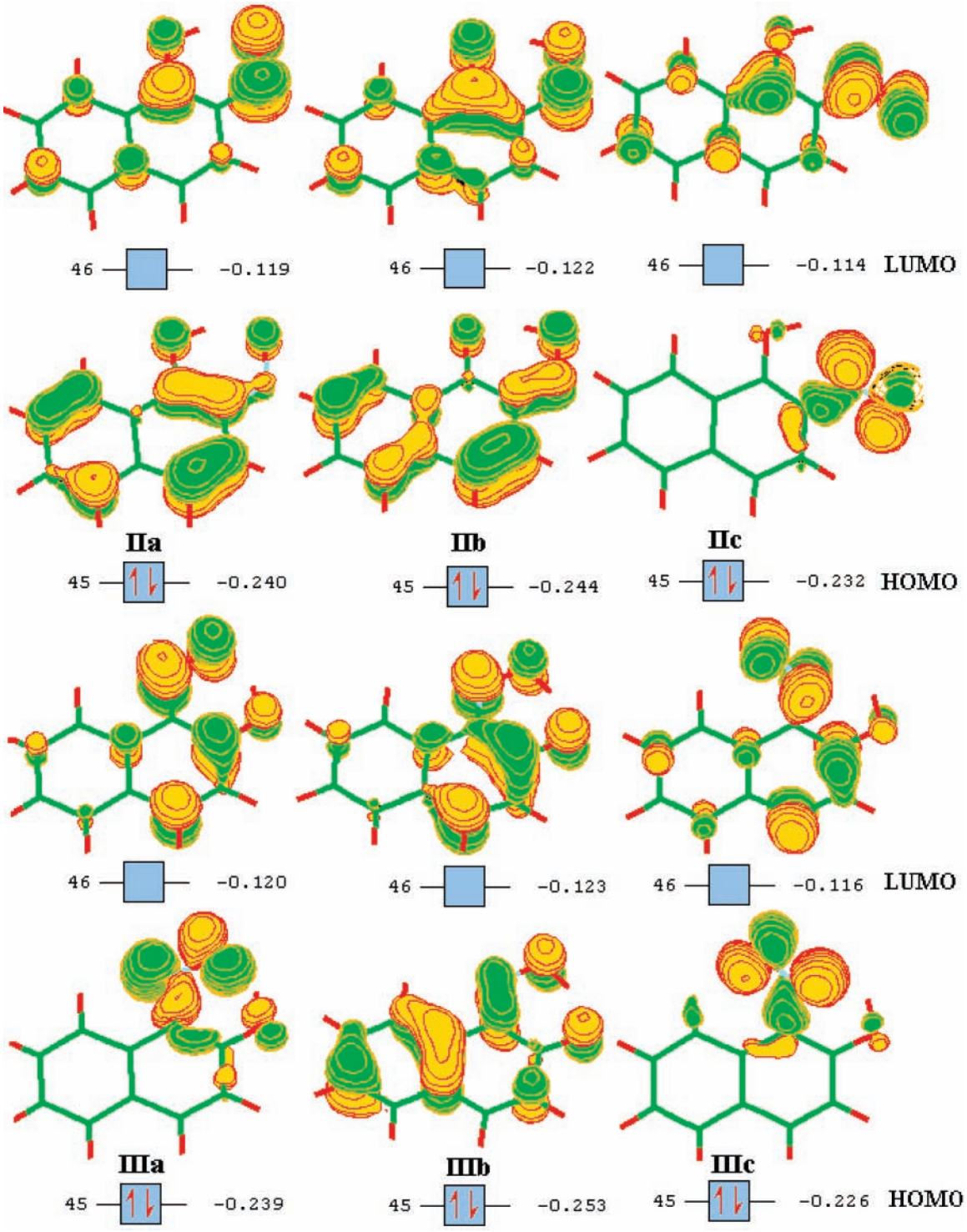

Figure 4. Schematic diagram of molecular orbitals with absolute orbital energies (a.u.) within B3LYP/6-311++G(d,p) computations for different forms of 2-nitroso-1-naphthol and 1-nitroso-2-naphthol.

was carried out with a correlation coefficient of 0.9662. Overall, the results of NBO analysis indicate that the intramolecular interactions are a stronger for monooxime tautomeric forms.

The topological analysis of Bader's theory is applied in this study. The AIM method was extended and implemented within the Gaussian program by Cioslowski.[35−37] The analysis of the bond critical points (BCP) for the O−H···O systems investigated here is given. The electron density at those BCPs (ρ_{BCP}), the Laplacian of that electron density ($\nabla^2\rho_{bcp}$) and the ellipticity are gathered in Table 7. The results of Table 7 are in the line with the above-mentioned AIM criteria of H bonding.[38] According to the H-bonding AIM-based criteria, the electronic density value at the BCP for the H-bonding should lie within the range 0.002−0.004.[39] The similar agreement with the AIM criteria is observed for our molecules. Another AIM criterion of H-bonding concerns the range of the values of the Laplacian of electronic density at BCP. It is 0.024−0.139 a.u.[40] Table 7 shows that all these values for H···O contacts $\nabla^2\rho_{bcp(0\cdots H)}$ for the systems explored here are within the abovementioned range. Thus it is visible that the AIM analysis based on ρ_{BCP} and $\nabla^2\rho_{BCP}$ values leads to the conclusion that the H bonds

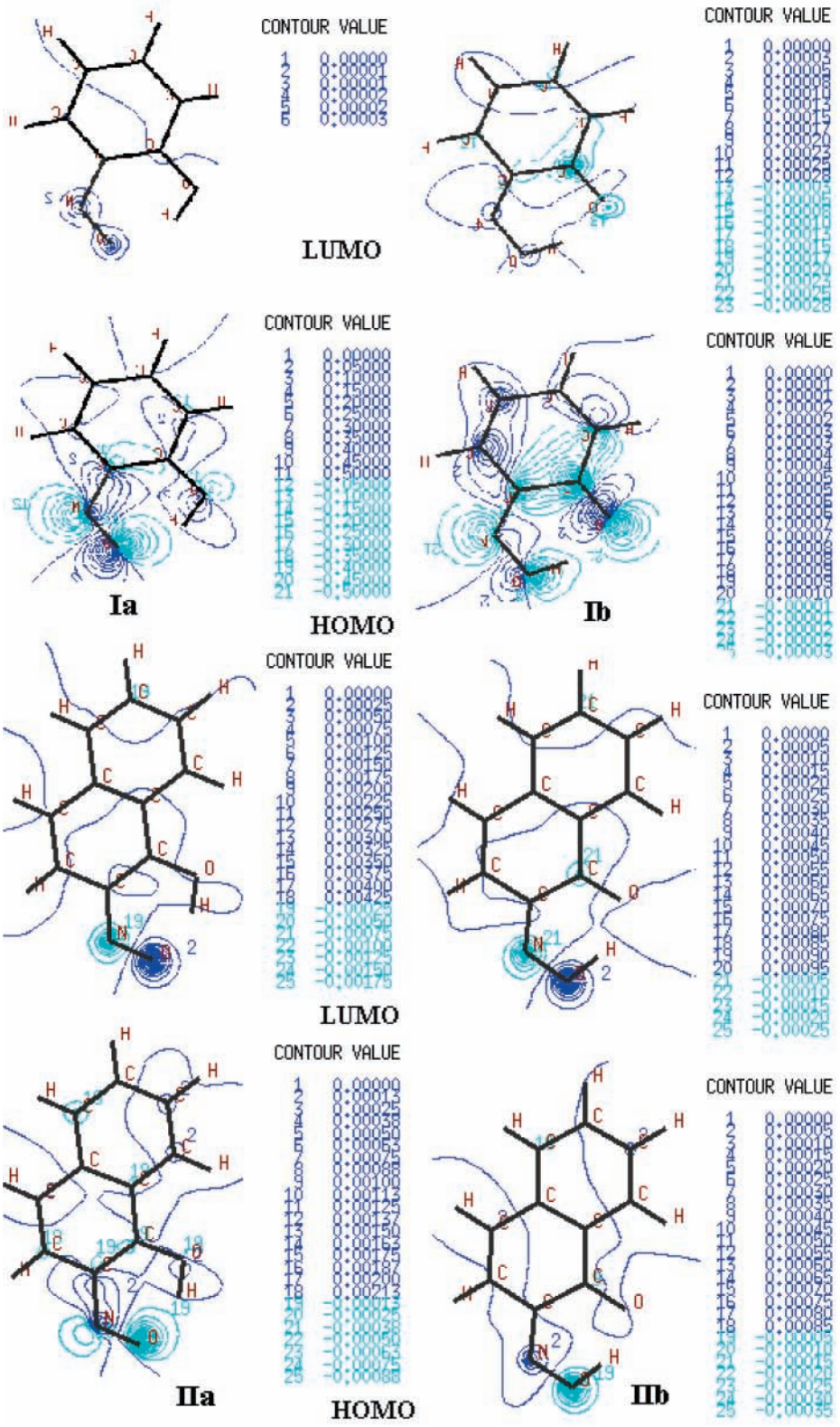

Figure 5. Contour map of electron density of HOMO and LUMO orbitals for different forms of 2-nitrosophenol and 2-nitroso-1-naphthol. The calculations are carried out at B3LYP/6-311++G(d,p) level. The contour values in a.u. are presented.

investigated here would correspond to strong HBs according to the classification.[41]

It is interesting to compare the electron density properties of O···H−O and N···H−O bonding in **Ia**, **Ib**, and **Ic**. The ρ_b(O···H) and ρ_b(N···H) values confirm the suggestion for stronger O···H hydrogen bond as compared to the N···H one. Similarly, data of O···H−O hydrogen bonding between **Ia** and **Ib** indicate the greater value of ρ_b(O···H) for **Ib** than for the **Ia** molecule is in agreement with the previous observations that the electron density at BCP of H-bond corresponds to its strength.

Also, analyzing of the data from Table 7, one can conclude that the ρ_{BCP} and $\nabla^2\rho_{BCP}$ decrease a few in passing from the gaseous phase to polar aqueous solution. Thus the strength of the hydrogen bonding is rather weakened in polar solution.

Recently it has been pointed out that the topological properties may be useful to describe the intermolecular and intramolecular

TABLE 6: B3LYP/6-311++G(d,p) NBO Analysis of Occupation Numbers for 2-Nitrosophenol and Nitrosonaphthols Including σ^*_X-H Antibonds, the Nature of Donor Orbitals ϕ_i, and Acceptor Orbitals ϕ

	$\sigma^*O_7-H_8$	$\sigma^*N_9-O_{10}$	$\sigma^*O_{10}-H_8$	$\phi_i \rightarrow \phi_j^*$ [b]	$\Delta E_{ij}^{(2)}$ [c]	ΔE_{DEL} [c]
Ia	0.063	0.006		LP(2) O10 → BD(1) O7−H8	20.87	35.435
	(0.058)	(0.007)		(LP(2) O10 → BD(1) O7−H8)	(18.87)	
Ib		0.014	0.099	LP(2) O7 → BD(1) O10−H8	38.82	80.346
		(0.015)	(0.095)	(LP(2) O7 → BD(1) O10−H8)	(37.09)	
M	0.024	0.006		LP(1) N9 → BD(1) O7−H8	2.85	10.053
	(0.015)	(0.006)		(LP(1) N9 → BD(1) O7−H8)	(1.41)	
IIa	0.087	0.007		LP(2) O10 → BD(1) O7−H8	32.11	49.364
	(0.082)	(0.008)		(LP(2) O10 → BD(1) O7−H8)	(30.18)	
IIb		0.014	0.080	LP(2) O7 → BD(1) O10−H8	28.97	68.289
		(0.017)	(0.078)	(LP(2) O7 → BD(1) O10−H8)	(28.42)	
IIc	0.028	0.006		LP(1) N9 → BD(1) O7−H8	3.72	11.642
	(0.018)	(0.006)		(LP(1) N9 → BD(1) O7−H8)	(1.67)	
IIIa		0.006		LP(2) O10 → LPa(1) H8	49.19	50.984
	(0.087)	(0.007)		(LP(2) O10 → BDa(1) O7−H8)	(33.54)	
IIIb		0.015	0.086	LP(2) O7 → BD(1) O10−H8	33.42	71.946
		(0.016)	(0.084)	(LP(2) O7 → BD(1) O10−H8)	(32.35)	
IIIc		0.007		LP(1) N9 → RYa(1) H8	8.49	14.800
		(0.008)		(LP(1) N9 → LPa(1) H8)	(4.51)	
IVa	0.053	0.006		LP(2) O10 → BD(1) O7−H8	16.50	30.049
	(0.048)	(0.007)		(LP(2) O10 → BD(1) O7−H8)	(15.04)	
IVc	0.022	0.006		LP(1) N9 → BD(1) O7−H8	2.86	10.092
	(0.015)	(0.006)		(LP(1) N9 → BD(1) O7−H8)	(1.38)	

[a] The same parameters for the studied compounds in aqueous solution are given in parentheses. [b] 1 is σ, 2 is π. [c] Second-order perturbation energy $\Delta E_{ij}^{(2)}$ and the energy change ΔE_{DEL} from the NBO energetic deletion analysis are given in kcal/mol.

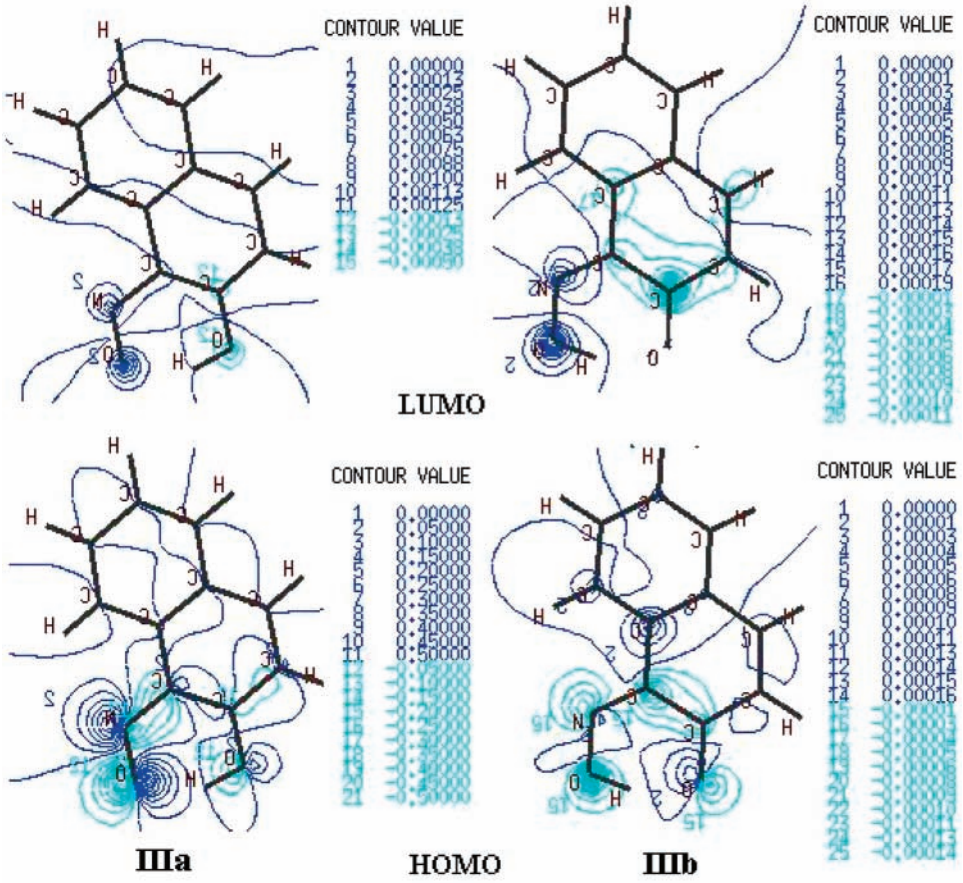

Figure 6. Contour map of electron density of HOMO and LUMO orbitals for different forms of 1-nitroso-2-naphthol. The calculations are carried out at B3LYP/6-311++G(d,p) level. The contour values in a.u. are presented.

H-bond strength.[42,43] In connection with above-mentioned, we have built the correlation ratio between the X···H distances and electron densities, Laplacian densities and ellipticities of possible IHBs formed in 2-nitrosophenol at the corresponding bond critical points according to the B3LYP/6-311++G(d,p) data. The linear regression line is shown in Figure 8. We may see that the electron density between the hydrogen atom and the proton acceptor decreases linearly with augmentation of the X···H distance. The analogous situation is observed at the correlation between X···H distances and Laplacian $\nabla^2\rho_b$ density. Also, we have received the correlation ratio between X···H distances and ellipticity. The correlation coefficients (r) were

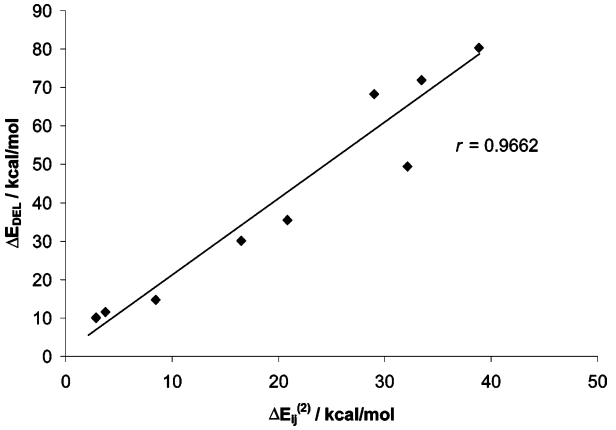

Figure 7. Correlation of the second-order perturbation energy $\Delta E_{ij}^{(2)}$ in **I**−**IV** (Table 6) with the energy change ΔE_{DEL} from the NBO energetic deletion analysis (B3LYP/6-311++G(d,p)).

0.9791, 0.9993, and 0.9749 for the first case, second, and third one, respectively. For the number of points equal to three, a difference of the correlation coefficient from zero is significant when it is strictly equal to unity. However, sufficiently high (r) value attests to the fact that the correlation obtained has a not random nature. Thus the above correlations demonstrate the connection of topological, spatial and geometry properties. Hence the Bader's topological theory may be useful for the evaluation of the H-bonding interactions from the electron density, and the properties of the BCPs are useful descriptors for the estimation the strengths of the intramolecular H bonds.

3.6. NMR Data Analysis. The GIAO[28−30] approach was used to calculate the absolute shielding constants for the tautomers and rotamers of 2-nitrosophenol and nitrosonaphthols in the gaseous phase and in water solution. The GIAO calculations were performed at B3LYP/6-311++G(d,p) level using optimized geometry at the same level of theory. The obtained results and available experimental data are listed in Table 8. As can be seen from this Table, the calculated chemical shifts for **IIb** and **IIIb** are in a good agreement with the experimental values.

The H_8 protons in conformers **Ib**, **IIb**, and **IIIb** are more shielded than those in the other ones. This may be ascribed to the stronger interaction between oxygen and hydrogen atoms. In comparison between conformers **Ib**, **IIb**, and **IIIb**, the chemical shifts of the proton H_8 in **Ib** is computed to be 18.8 ppm, which is about 1 ppm larger than that in **IIb** and **IIIb**. Also, the H_8 protons in **Ia**, **Ib**, **IIa**, **IIb**, **IIIa**, **IIIb**, and **IVb** are a few positive shielded in the gaseous phase as compared with solution than conformers without hydrogen-bonded interaction. In all the cases, the ^{1}H chemical shifts are on the order of 8−19 ppm and lie in agreement with a hydrogen bonding interaction, and the values of ^{1}H would correspond to strong IHBs according the classification.[44]

The chemical shift of the O_{10} has a large positive value in all oxime tautomeric forms and shows a large negative value for all nitroso ones. It may testify that that chemical shift increase with increasing negative charge at O_{10} (Table 4). As to O_7 atom, there is a large positive chemical shift during the process (**Xa** → **Xb**, **X** = **I**−**III**) for the gaseous phase and water solution.

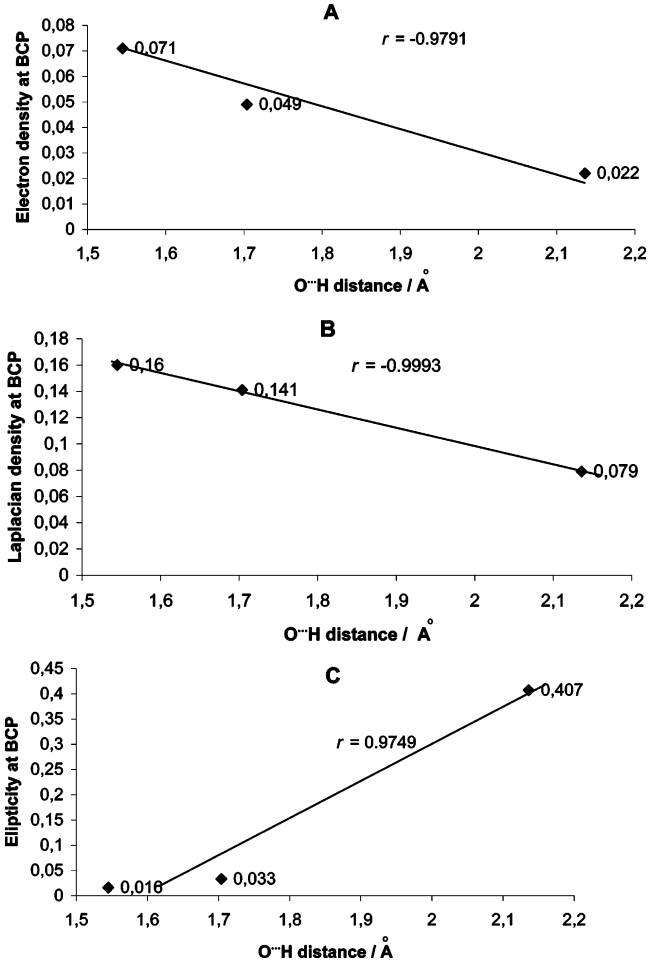

Figure 8. Correlation of O···H distances in 2-nitrosophenol with (A) electron density at BCPs, (B) electron density Laplacian ($\nabla^2\rho$) at BCPs, and (C) ellipticity at BCPs (B3LYP/6-311++G(d,p)).

In this study we have received the correlation equations of the O−H···O hydrogen bonds distances with ^{1}H chemical shifts calculated at B3LYP/6-311++G(d,p) level in the gaseous phase and aqueous solution. The linear regression lines are shown in Figure 9. It can be see that the ^{1}H chemical shifts increase linearly with decrease of the O···H distance. The correlation coefficients (r) were 0.9784 for the gaseous phase and 0.9901 for the aqueous solution. Thereby the above linear relationships demonstrate the connection of NMR spectroscopic properties and geometry. Hence, the obtained correlation may be effective for the strength evaluation of the H-bonding interactions from NMR analysis.

TABLE 7: Electron Density (ρ_{BCP}), Laplacian ($\nabla^2\rho_{\mathrm{BCP}}$), and Ellipticity Calculated at the BCPs of the Possible IHBs Formed in Different Forms of 2-Nitrosophenol Calculated by the B3LYP/6-31 1++G(d,p) Method[a]

	$\rho_{\mathrm{BCP(O\cdots H)}}$		$\nabla^2\rho_{\mathrm{BCP(O\cdots H)}}$		ellipticity		d(H···X)		a(X−H···Y)	
	A[b]	B[b]	A	B	A	B	A	B	A	B
Ia	0.049	0.046	0.141	0.138	0.033	0.034	1.704	1.723	143.646	142.094
Ib	0.071	0.069	0.160	0.160	0.016	0.019	1.545	1.554	151.471	150.825
Ic	0.022	0.018	0.079	0.077	0.407	0.406	2.136	2.281	114.703	107.979

[a] The distance (d, Å) and angle (a, deg) of such interactions are also included. [b] A, in the gaseous phase (B3LYP/6-311++G(d,p); B, in the solvent, SCRF (PCM, solvent = water).

TABLE 8: GIAO B3LYP/6-311++G(d,p) Calculated ^{1}H, ^{13}C, ^{15}N, and ^{17}O NMR Chemical Shifts for the Tautomers and Rotamers of 2-Nitrosophenol and Nitrosonaphthols Using B3LYP/6-311++G(d,p) Optimized Geometries (Numbering of the Atoms in Figure 1; Experimental Values,[10] in $CHCl_3$, in Brackets)

atom	**Ia**	**Ia** in solution[a]	**Ib**	**Ib** in solution[a]	**Ic**	**Ic** in solution[a]	**Id**	**Id** in solution[a]	**Ie**	**Ie** in solution[a]
O_{10}	−737. 0	*−578.6*	288.5	*330.2*	−1090. 7	*−864.6*	−1384. 6	*−1032.6*	302.4	*326.0*
N_9	−446. 8	*−383.3*	−40.3	*−4.5*	−460.8	*−437.7*	−591.0	*−509.2*	47.8	*34.2*
O_7	77.8	*96.6*	226.16	*250.1*	101.1	*116.2*	117.8	*132.7*	−31.6	*76.1*
H_8	13.1	*13.0*	18.8	*18.4*	11.1	*11.3*	3.8	*7.4*	8.6	*8.5*
C_1	148.2	*150.6*	183.9	*181.5*	175.2	*176.6*	134.1	*140.1*	181.6	*183.2*
C_2	166.4	*169.1*	158.8	*159.9*	163.2	*168.3*	162.2	170.7	155.3	*157.3*
	IIa	**IIa** in solution[a]	**IIb**	**IIb** in solution[a]	**IIc**	**IIc** in solution[a]	**IId**	**IId** in solution[a]	**IIe**	**IIe** in solution[a]
O_{10}	−587. 9	*−412.8*	316.5	*291.4*	−989.9	*−740.4*	−1424. 4	*−1023.2*	290.9	*304.5*
N_9	−391. 4	*−315.3*	−9.2	*30.8*	−404.4	*−372.5*	−604.8	*−501.8*	58.8	*56.9*
O_7	79.2	*106.5*	208.7	*225.0*	100.5	*122.0*	101.8	*122.2*	14.9	*91.3*
H_8	16.1	*16.0*	17.5 (17.0)	*17.2*	12.2	*12.2*	5.4	*8.3*	8.3	*11.0*
C_1	147.4	*152.5*	182.8 (182.2)	*183.2*	175.4	*177.9*	122.9	*132.6*	180.6	*183.9*
C_2	162.2	*164.7*	155.3 (147.1)	*157.3*	160.1	*164.8*	155.5	*166.2*	153.6	*155.5*
	IIIa	**IIIa** in solution[a]	**IIIb**	**IIIb** in solution[a]	**IIIc**	**IIIc** in solution[a]	**IIId**	**IIId** in solution[a]	**IIIe**	**IIIe** in solution[a]
O_{10}	−571. 7	*−371.7*	305.3	*285.3*	−997.9	*−749.7*	−1478. 4	*−1024.7*	279.2	*295.8*
N_9	−379. 7	*−300.6*	2.9	*33.91*	−412.5	*−374.3*	−626.9	*−513.1*	72.0	*61.7*
O_7	81.6	*109.6*	193.0	*224.8*	118.8	*136.9*	116.2	*138.7*	−26.6	*75.1*
H_8	16.3	*16.4*	17.9 (17.4)	*17.7*	12.1	*12.0*	3.8	*7.8*	8.2	*11.0*
C_1	149.2	*154.7*	181.8 (182.8)	*178.9*	180.2	*181.9*	124.2	*134.6*	182.0	*182.2*
C_2	159.9	*162.6*	152.8 (144.8)	*154.9*	156.0	*159.9*	152.5	*163.5*	150.1	*152.0*
	IVa	**IVa** in solution[a]	**IVb**	**IVb** in solution[a]	**IVc**	**IVc** in solution[a]	**IVd**	**IVd** in solution[a]	**IVe**	**IVe** in solution[a]
O_{10}	−812. 3	*−643.9*			−1162. 4	*−940.5*	−1375. 5	*−1047.9*	317.6	*313.2*
N_9	−468. 1	*−404.0*			−496.3	*−471.4*	−580.5	*−510.3*	36.6	*12.2*
O_7	77.4	*89.6*			98.1	*106.0*	113.2	*120.9*	−26.5	*113.5*
H_8	11.3	*11.1*			11.0	*10.8*	3.9	*7.1*	9.1	*12.3*
C_1	147.9	*148.7*			168.9	*169.0*	140.0	*142.9*	180.5	*182.3*
C_2	164.7	*167.8*			161.3	*165.7*	161.2	*169.6*	156.2	*158.4*

[a] SCRF PCM method.

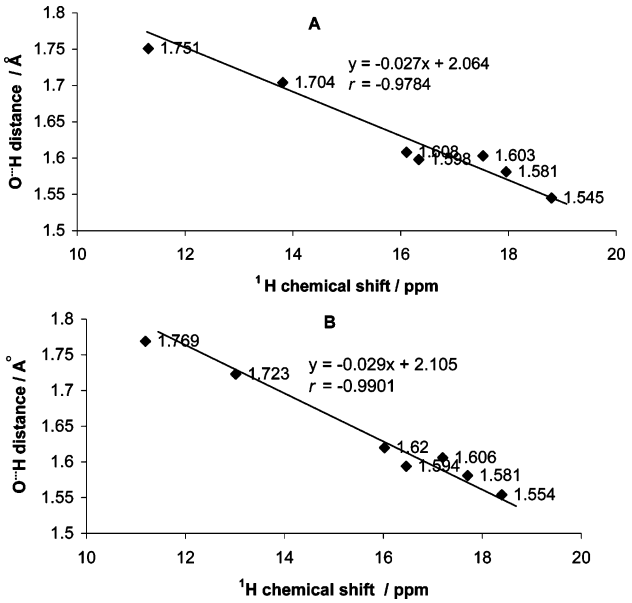

Figure 9. Correlation of O···H distances in **Ix**−**IVx** (x = a, b) with ^{1}H chemical shift. (A) Gaseous phase; (B) aqueous solutions.

4. Conclusion Remarks

The molecular structure and the nature of IHB for different species of 2-nitrosophenol and nitrosonaphthols are theoretically investigated at ab initio and DFT level of theory. The calculations performed in this paper show that for these systems, the similar effects exist as for typical O−H···O hydrogen bonds. In this paper we have applied PCM method to study the solvent effects on conformational geometry, IHB energy formation, charge distributions, AIM properties, and selected NMR chemical shifts. The hydrogen bond energy formation for nitroso tautomeric forms is larger than for oxime ones. The analysis of charge density has shown that all the systems studied here satisfy the indicative criteria of hydrogen bonding interactions. Careful conformational analyses of given molecules show that both that the size and charge differences between oxygen atoms in these compounds are very important factors not only for comparing their conformational behavior but also for understanding the nature of hydrogen bonding. Besides, good correlations between O···H distance and the difference of charge density ($Q_H - Q_A$), electron density at BCP, Laplacian density at BCP, and ellipticity has been found.

The results of NBO analysis indicate that interactions in nitroso forms are stronger than those in oxime ones (except for **Ia** and **Ib**). The hydrogen bond is stronger in the *syn*-oxime structure **Ib** of 2-nitrosophenol than that of the others, especially in aqueous medium. The results of this study also show that the topological parameters may be applied to estimate the H-bond strength. The NMR ^{1}H chemical shifts may be useful descriptors for the strength of intramolecular H-bonds.

Supporting Information Available: Table of energies. This material is available free of charge via the Internet at http://pubs.acs.org.

References and Notes

(1) Jeffrey, G. A. *An Introduction to Hydrogen Bonding*; Oxford University Press: New York, 1997.

(2) Hibbert, F.; Emsley, J. *Adv. Phys. Org. Chem.* **1990**, *26*, 255.

(3) Maistrenko, V. N.; Hamitov, R. Z.; Budnikov, G. K. *An Ecological and Analytical Monitoring of Superecotoxicants*; Khimiya: Moscow, 1996.

(4) Krzan, A.; Crist, D. R.; Horák, V. *J. Mol. Struct. Theochem.* **2000**, *258*, 237.
(5) Shono, T.; Hayashi, Y.; Shinra, K. *Bull. Chem. Soc. Jpn.* **1971**, *44*, 3179.
(6) Shpinel, Ya. I.; Tarnopol'skii,Yu. I. *Zh. Organ. Khim*. **1977**, *13*, 1030.
(7) Bartulin, J.; Belmar, J.; Gallardo, H.; Leon, G. *J. Heterocycl. Chem*. **1994**, *31*, 561.
(8) Enchev, V.; Ivanova, G.; Ugrinov, A.; Neykov, G. D.; Minchev, St.; Stoyanov, N. *J. Mol. Struct.* **1998**, *440*, 227.
(9) Enchev, V.; Ivanova, G.; Ugrinov, A.; Neykov, G. D. *J. Mol. Struct.* **1999**, *508*, 149.
(10) Ivanova, G.; Enchev, V. *Chem. Phys.* **2001**, *264*, 235.
(11) Ivanova, G.; Abrahams, I.; Enchev, V. *J. Mol. Struct.* **2002**, *608*, 193.
(12) Enchev, V.; Ivanova, G.; Stoyanov, N. *J. Mol. Struct. (THEOCHEM)* **2003**, *640*, 149.
(13) Enchev, V.; Stoyanov, N; Ivanova, G.; *Proceedings Ruse University* **2001**, *38*, 196.
(14) Frisch, M. J.; Trucks, G. W.; Schlegel, H. B.; Scuseria, G. E.; Robb, M. A.; Cheeseman, J. R.; Zakrzewski, V. G.; Montgomery, J. A.; Stratmann, R. E.; Burant, J. C.; Dapprich, S.; Millan, J. M.; Daniels, A. D.; Kudin, K. N.; Strain, M. C.; Farkas, O.; Tomasi, J.; Barone, V.; Cossi, M.; Cammi, R.; Mennucci, B.; Pomelli, C.; Adamo, C.; Clifford, S.; Ochterski, J.; Petersson, G. A.; Ayala, P. Y.; Cui, Q.; Morokuma, K.; Malich, D. K.; Rabuck, A. D.; Raghavachari, K.; Foresman, J. B.; Cioslowski, J.; Ortiz, J. V.; Baboul, A. G.; Stefanov, B. B.; Liu, G.; Liashenko, A.; Piskorz, P.; Komaromi, I.; Gomperts, R.; Martin, R. L.; Fox, D. J.; Keith, T.; Al-Laham, M. A.; Peng, C. Y.; Nanayakkara, A.; Gonzales, C.; Challacombe, M.; Gill, P. M. W.; Johnson, B.; Chen, W.; Wong, M. W.; Andreas, J. L.; Head-Gordon, M.; Reploge, E. S.; Pople, J. A. *Gaussian 98*, revision A.7; Gaussian, Inc.: Pittsburgh, PA 1998.
(15) Frisch, M. J.; Trucks, G. W.; Schlegel, H. B.; Scuseria, G. E.; Robb, M. A.; Cheeseman, J. R.; Zakrzewski, V. G.; Montgomery, J. A.; Stratmann, R. E.; Burant, J. C.; Dapprich, S.; Millan, J. M.; Daniels, A. D.; Kudin, K. N.; Strain, M. C.; Farkas, O.; Tomasi, J.; Barone, V.; Cossi, M.; Cammi, R.; Mennucci, B.; Pomelli, C.; Adamo, C.; Clifford, S.; Ochterski, J.; Petersson, G. A.; Ayala, P. Y.; Cui, Q.; Morokuma, K.; Malich, D. K.; Rabuck, A. D.; Raghavachari, K.; Foresman, J. B.; Cioslowski, J.; Ortiz, J. V.; Baboul, A. G.; Stefanov, B. B.; Liu, G.; Liashenko, A.; Piskorz, P.; Komaromi, I.; Gomperts, R.; Martin, R. L.; Fox, D. J.; Keith, T.; Al-Laham, M. A.; Peng, C. Y.; Nanayakkara, A.; Gonzales, C.; Challacombe, M.; Gill, P. M. W.; Johnson, B.; Chen, W.; Wong, M. W.; Andreas, J. L.; Head-Gordon, M.; Reploge, E. S.; Pople, J. A. *Gaussian 03*, revision B-03; Gaussian, Inc.: Pittsburgh, PA 2003.
(16) Becke, A. D. *J. Chem. Phys.* **1993**, *98*, 5648.
(17) Lee, C.; Yang, W.; Parr, R. G. *Phys. Rev. B* **1988**, *37*, 785.
(18) Lynch, B. J.; Fast, P. L.; Harris, M.; Truhlar, D. G. *J. Phys. Chem*. **2000**, *A104*, 4811.
(19) Schlegel, H. B.; McDouall, J. J. In *Computational Advances in Organic Chemistry*; Ogretir, C., Csizmadia, I. G., Eds.; Kluwer Academic: The Netherlands, 1991; p 167.
(20) Ditchfield, R.; Hehre, W. J.; Pople, J. A. *J. Chem. Phys.* **1971**, *54*, 724.
(21) McLean, A. D.; Chandler, G. S. *J. Chem. Phys.* **1980**, *72*, 5639.
(22) Krishnan, R.; Binkley, J. S.; Seeger, R.; Pople, J. A. *J. Chem. Phys.* **1980**, *72*, 650.
(23) Glendening, E. D.; Reed, A. E.; Carpenter, J. E.; Weinhold, F. A. *NBO Version* **1995**, *3.1*.
(24) Bader, R. F. W. *Atoms in Molecules: A Quantum Theory*; Clarendon Press: Oxford, 1990.
(25) Tapia, O. In *Molecular Interaction*; Ratajczak, H., Orville-Thomas, W. J., Eds.; Wiley: New York, 1982; Vol. 3, p 47.
(26) Amovilli, C.; Barone, V.; Cammi, R.; Cances, E.; Cossi, M.; Mennucci, B.; Pomelli, C. S.; Tomasi, J. *Adv. Quantum Chem.* **1998**, *32*, 227.
(27) Barone, V.; Cossi, M.; Mennucci, B.; Tomasi, J. *J. Chem. Phys.* **1997**, *107*, 3210.
(28) Wolinski, K.; Hilton, J. F.; Pulay, P. *J. Am. Chem. Soc.* **1990**, *112*, 251.
(29) Dodds, J. L.; McWeeny, R.; Sadlej, A. J. *Mol. Phys*. **1980**, *41*, 1419.
(30) Ditchfield, R. *Mol. Phys.* **1974**, *27*, 789.
(31) Zefirov, U. V.; Zorkii, P. M. *Usp. Khim.* **1995**, *64*, 446.
(32) Frey, A. *Magn. Reson. Chem.* **2001**, *39*, 190.
(33) Buemi, G. *Chem. Phys.* **2002**, *277*, 241.
(34) Reed, A. E.; Curtiss, L. A.; Weinhold, F. A. *Chem. Rev.* **1988**, *88*, 899.
(35) Cioslowski, J.; Nanayakkara, A.; Challacombe, M. *Chem. Phys. Lett.* **1993**, *203*, 137.
(36) Cioslowski, J.; Mixon, S. T. *J. Am. Chem. Soc.* **1991**, *113*, 4142.
(37) Cioslowski, J. *Chem. Phys. Lett.* **1994**, *219*, 151.
(38) Koch, U.; Popelier, P. *J. Phys. Chem.* **1995**, *99*, 9747.
(39) Popelier, P. *Atoms in Molecules*; Prentice Hall: Perason Education Ltd, 2000; p 150.
(40) Popelier, P. *J. Phys. Chem.* **1998**, *102*, 1873.
(41) Rozas, I.; Alkorta, I.; Elguero, J. *J. Am. Chem. Soc*. **2000**, *122*, 11154.
(42) Quiñonero, D.; Frontera, A.; Ballester, P.; Garau, C.; Costa, A.; Deyá, P. M. *Chem. Phys. Lett.* **2002**, *133*, 1373.
(43) Grabowski, S. J. *Monatsh. Chem.* **2002**, *133*, 1373.
(44) Hibbert, F.; Emsley, J. *Adv. Phys. Org. Chem*. **1990**, *26*, 255.
(45) Soundararajan, S.; Vold, M. J. *Trans Faraday Soc.* **1958**, *54*, 1155.